IJEPS 3 (3): 51-62 (2020)

Studying the Effect of Substituting Praseodymium in Superconductor ($YBa_2Cu_3O_{7-\delta}$)

Afaf S. Zawaly[1], Someraa S. Shakonah[2], Hanan A. Altahir[3]

Zawia University, College of Education, Abu-Issa, Physics Department, Zawia, Libya

Corresponding Emails: a.zawaly@zu.edu.ly[1]; s.shakonah@zu.edu.ly[2]; h.abdulrahman@zu.edu.ly[3]

Superconductors are materials that lose all resistance to the flow of electricity when cooled below a critical transition temperature (Tc) however; this ability of superconductors to conduct electricity with zero resistance can be exploited in the use of electrical transmission lines. Bulk high-temperature superconductors (HTS) exhibits lower critical current densities than thin films which result of the weak superconductivity at the grain boundaries. The critical current rapidly falls with respect to applied magnetic field than with thin films. Superconductivity is a thermodynamic phase distinguishing properties that depends on microscopic details such as zero resistivity to low applied currents in the absence of magnetic field or at an applied field less than the critical value. The uniqueness of high temperature superconductor relies much on their ability to maintain steady current and expel magnetic fields effect without deteriorating. The aim of this research is to investigate the effect of Pr substitution in the (YBa_2 Cu_3-x Prx) $O_{7-\delta}$ (x= 0, 0.1, 0.2, 0.3) and metallic behavior over the range of samples.

Keywords: Praseodymium, superconductor ($YBa_2Cu_3O_{7-\delta}$), lattice parameters, thermodynamic

1. Introduction

Superconductors are materials that lose all resistance to the flow of electricity when they cooled below a critical transition temperature (T_c) however; this ability of superconductors to conduct electricity with zero resistance can be exploited in the use of electrical transmission lines. Reasonable fraction of electrical energy is lost in form of heat through resistance, associated with traditional conductors such as copper and aluminum [1]. However, the advances in superconductivity technology depend on the ease with which wires can be prepared from the brittle ceramics that retain their superconductivity at 77 K that supports large current densities. The behavior of electrons is vastly different inside a superconductor. The presence of impurities and lattice affect the movement of the superconducting electrons however, as the superconducting electrons travel through the conductor they pass unobstructed through the complex lattice [2]. Because they bump into nothing and create no friction they can transmit electricity with no appreciable loss in the current and no loss of energy.

$YBa_2Cu_3O_{7-\delta}$ was the first high temperature superconductor (HTS) compound with T_c above the temperature of liquid nitrogen [3]. With the application of pressure on its optimal doping state ($\delta \approx 0.05$, $T_c = 93$ K), a negligible increasing effect on δ, $YBa_2Cu_3O_{7-\delta}$, becomes under-doped with oxygen vacancies in the CuO chains T_c [4]. As a result of strong electrostatic potential, the mobile oxygen interacts with the holes' distribution in the CuO_2 planes and with cationic dopants of different valence. Changes in T_c of YBCO with re-distributed oxygen chains were explained by a charge transfer to the active CuO_2 layers that depends sensitively on the specific oxygen configuration [5]. This charge transfer also affects the electrical transport properties in the normal state. Superconductors can make energy production more efficient by reducing losses. The time-relaxation of the electrical resistivity of $YBa_2Cu_3O_{7-\delta}$ observed after hydrostatic pressure was applied at room temperature followed exactly the same stretched exponential relaxation function as the corresponding data for T_c with very similar relaxation times, activation energies, and migration volumes [6]. Correlation between the relaxation of T_c and that of the normal-state resistivity provides evidence for the common origin of both effects. Superconductors are subdivided into two types (type I and type II) depending on their magnetic behavior.

In application, superconducting magnets could be made smaller than a resistive magnet because the windings could carry large currents with no energy loss [7]. Since there is no loss in

electrical energy when superconductors carry electrical current, narrow wires made of superconducting materials could be employed to carry huge currents though there is a certain maximum current that these materials can be made to carry, above which they stop being superconductors. In the other hand, generators wound with superconductors could generate the same amount of electricity with smaller equipment and less energy and distributed through superconducting wires [8]. Energy could be stored in superconducting coils for long periods of time without significant loss. As long as the superconductor is cooled to very low temperatures, the cooper pairs stay intact, due to the reduced molecular motion. As the superconductor gains heat energy the vibrations in the lattice become more violent and break the pairs however, superconductivity diminishes as they break. Superconducting metals and alloys have characteristic transition temperatures from normal conductors [9].

2. Methodology

All the materials used in this experiment were purchased from Aldrich Sigma and stored at ambient temperature without further purification. Samples were prepared by solid state reaction via thoroughly mixed specific amount of high purity cation oxides of Y_2O_3 (99.99%), Pr_6O_{11} (99.99%), BaO (99.99%), and CuO (99.99%) were weighted and mixed according to the following chemical formula shown below.

$$1/2\ (Y_2O_3) + 2\ (BaO) + (3 - x)\ (CuO) + x/6\ (Pr_6O_{11}) \rightarrow YBa_2\ (Cu_{3-x}\ Pr_x)\ O_{7-\delta}$$

With x = 0, 0.1, 0.2, and 0.3.

Each of these mixtures was ground for one hour. They were put into a furnace and heated at 890 C^o in air for 24 hours followed by furnace cooling to room temperature. The powders were reground and put into the furnace and heated at 890 C^o in air for 24 hours followed by furnace cooling to room temperature. The resultant powders were reground and pressed into pellet. The pellets were then put into the furnace and heated at 890 C^o for 24 hours in air. Room temperature resistivity Schematic of **Van der Pauw** configurations have been used to determine the resistivity at room temperature. The sample was fixed onto a sample holder with silver paint. Digital voltmeter and multi-meter were used to record the voltage and resistance respectively. The room temperature resistivity ρ was computed using equation 1.

$$\rho = \frac{\pi d\, V_{CD}}{\ln 2\, I_{AB}} \qquad (1)$$

where d is the thickness of the sample, VCD is the voltage between the points C and D and IAB is the current through point A to B. The error was calculated by using the following equation:

$$\frac{\Delta\rho}{\rho} = \frac{\Delta d}{d} + \frac{\Delta V}{V} + \frac{\Delta I}{I} \qquad (2)$$

The superconducting properties such as the electrical resistance-temperature at zero temperature with variation praseodymium concentration *x* and the electrical resistance-temperature at T_c for samples were measured by four-point probe technique using silver paint contacts in conjunction with a closed cycle refrigerator from CTI Cryogenics Model 22. The temperature was cooled down at a cooling rate of 60 ^oC per hour and heated up with the same rate**.** The resistance and temperature were recorded and plotted as graphs with a normalized resistance versus temperature. In addition, the two-point probe method was used for samples that contained less than 0.60 vol. fraction of the superconducting material since the composites have high dc resistance. X-ray diffraction has been in use in two main areas, for the fingerprint characterization of crystalline materials and the determination of their structure. Each crystalline solid has its unique characteristic X-ray powder pattern which may be used as a "fingerprint" for its identification. We can determine the size and the shape of the unit cell for any compound most easily using the diffraction of x-rays**.**

The path difference between two waves:

$$2 \times \lambda = 2d\ Sin\ \theta \qquad (3)$$

For constructive interference between these waves, the path difference must be an integral number of wavelengths:

$$\lambda \times n = 2 \times\ x \qquad (4)$$

This leads to the Bragg equation:

$$\mathrm{n} \times \lambda = 2\mathrm{d}\ \mathrm{Sin}\ \theta \qquad (5)$$

The samples used for structural characterization were ground into powder. The powder was gently pressed into a standard sample holder and carefully serrated with blade of razor to make a smooth surface and also to minimize any possible preferred orientation in the specimen. The diffraction

data for the analysis were collected at room temperature ~298 K with a Siemens D5000 powder diffractometer. X-ray powder diffraction with CuKα radiation (XRD) with λ=1.541 A was employed to confirm the formation of the Y123 phase. The samples were scanned from 2^o-60^o, using a nickel filtered CuK_α source and silicon standard. The reading was taken for every 0.025^o. Scanning electron microscopy (SEM) was use to investigate the micro-structural properties of the composites at different cross-section. The cross-section surface of the sample was coated with evaporated gold prior to insertion into the sample chamber. Scanning electron micrographs were recorded using a Philips XL30 scanning electron microscope.

3. Results and Discussion

We investigated the effect of Pr_x on microstructure. Series of YBa_2 $(Cu_{1-x}Pr_x)_3O_{7-\delta}$ samples synthesized using conventional solid state reaction were characterized by means of X-ray diffraction and scanning electron microscopy. The grain size of the sample decrease with increase in Pr concentration. For x = 0, 0.1, 0.2, and 0.3 the grained size was 2.0μm, 1.5 μm, 1.12 μm and 1.14 μm respectively. Owing to the orthorhombic layered perovskite-like structure containing CuO_2 planes which accommodate the mobile holes is believed to be involved in the superconductivity. Pr is essentially trivalent with $PrBa_2Cu_3O_7$. Its substitution effect in the YBa_2 $(Cu_{3-x}$ $Pr_x)$ $O_{7-\delta}$ (x=0, 0.1, 0.2, 0.3) shows that Pr^{3+} is relatively stable and inhibit superconductivity through oxidation reduction reaction with the CuO bands. The effect of Pr is two folds; first it dopes the CuO_2 planes with electrons, countervailing the effect of the role of BaO, second it has a magnetic moment interaction with the conduction electrons sharply inhibits superconductivity. $PrBa_2Cu_3O_7$ is the only non-superconductor among the rare earth elements.

3.1. YBa_2 $(Cu_{3-x}Pr_x)$ $O_{7-\delta}$ phase

The powder X-ray diffraction patterns of $YBa_2Cu_{3-x}Pr_xO_{7-\delta}$ with x = 0, 0.1, 0.2 and 0.3 are shown in Figures 1-4, respectively. Characteristic peaks corresponding to different phases are marked on different patterns. The structural parameters obtained from the diffraction line of the entire samples possess orthorhombic perovskite like 1:2:3 layered structure. The XRD pattern corresponds to sample with x = 0, 0.1, 0.2, and 0.3 indicates a predominately single phase perovskite based orthorhombic and an insignificant amount of Pr as secondary phase compared with XRD for pure

sample. Figures 1 and 2 show the XRD patterns for the $YBa_2Cu_{3-x}Pr_xO_{7-\delta}$ with x ranging from 0 to 0.3 have the layered orthorhombic perovskite like structure.

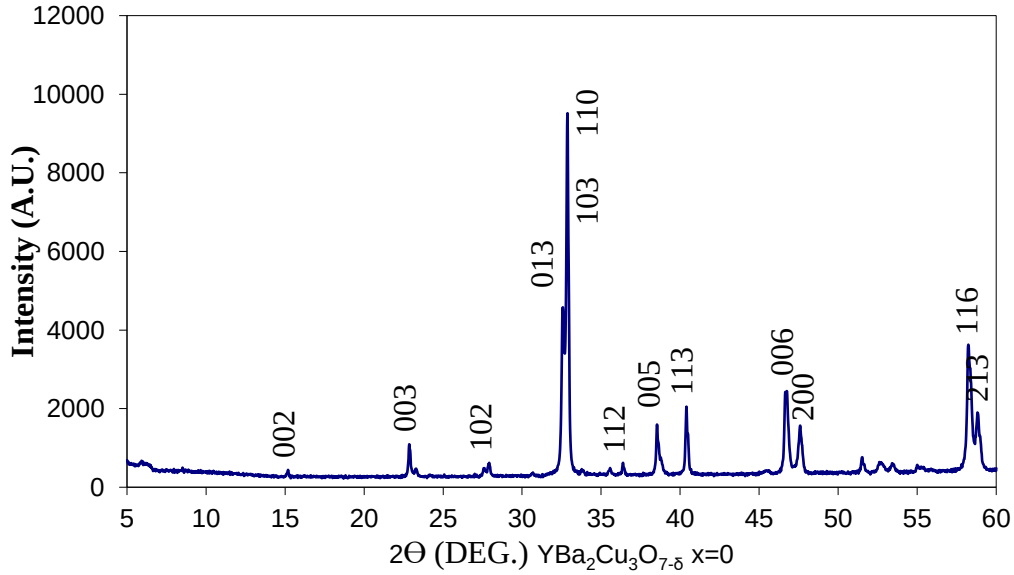

a

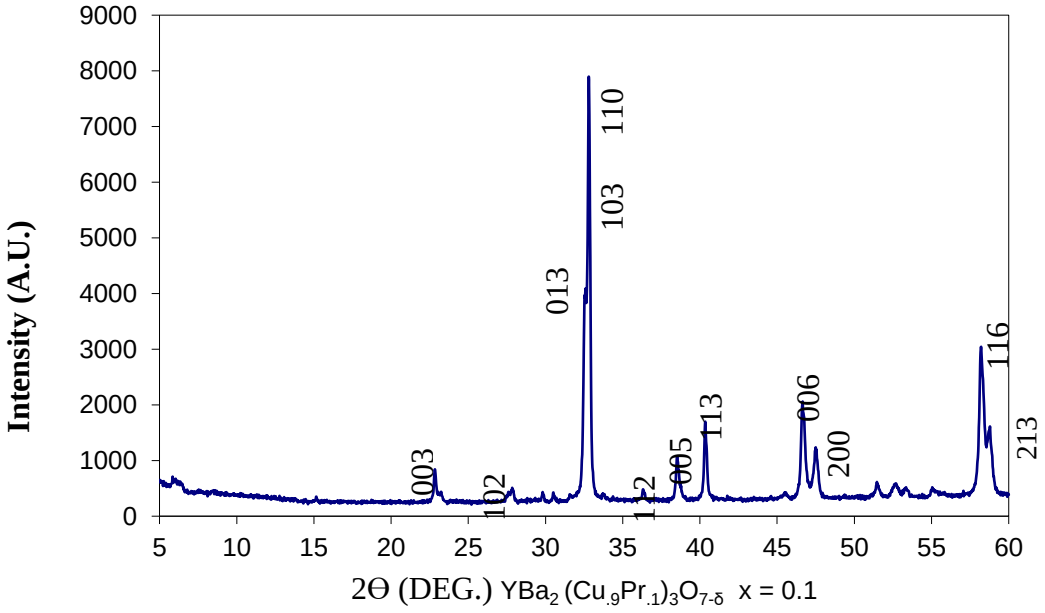

b

Figure 1 The X-ray powder diffraction pattern using Cu-K_α radiation of a: $YBa_2Cu_3O_{7-\delta}$ (x=0), b: $YBa_2(Cu_{.9}Pr_{.1})_3O_{7-\delta}$ (x = 0.1)

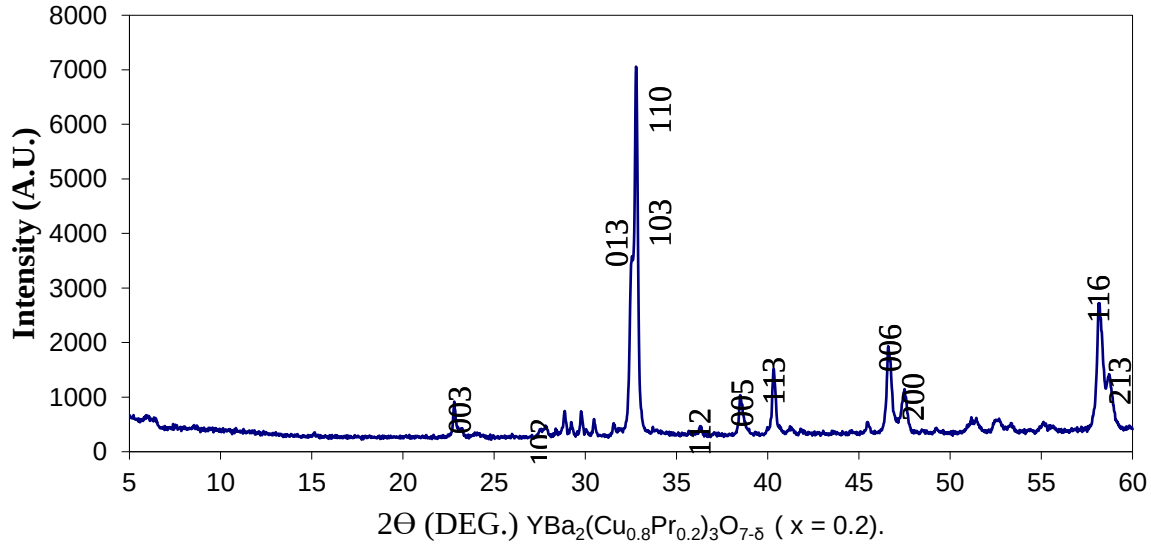

a

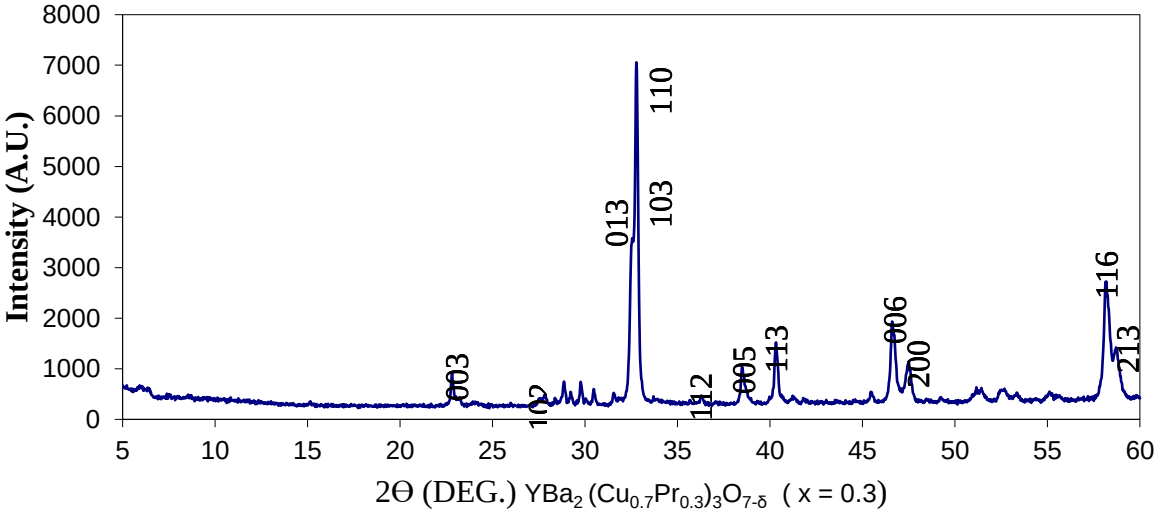

b

Figure 2 The X-ray powder diffraction pattern using Cu-K_α radiation of a: $YBa_2(Cu_{0.8}Pr_{0.2})_3O_{7-\delta}$ (x = 0.2) and b: $YBa_2(Cu_{0.7}Pr_{0.3})_3O_{7-\delta}$ (x = 0.3)

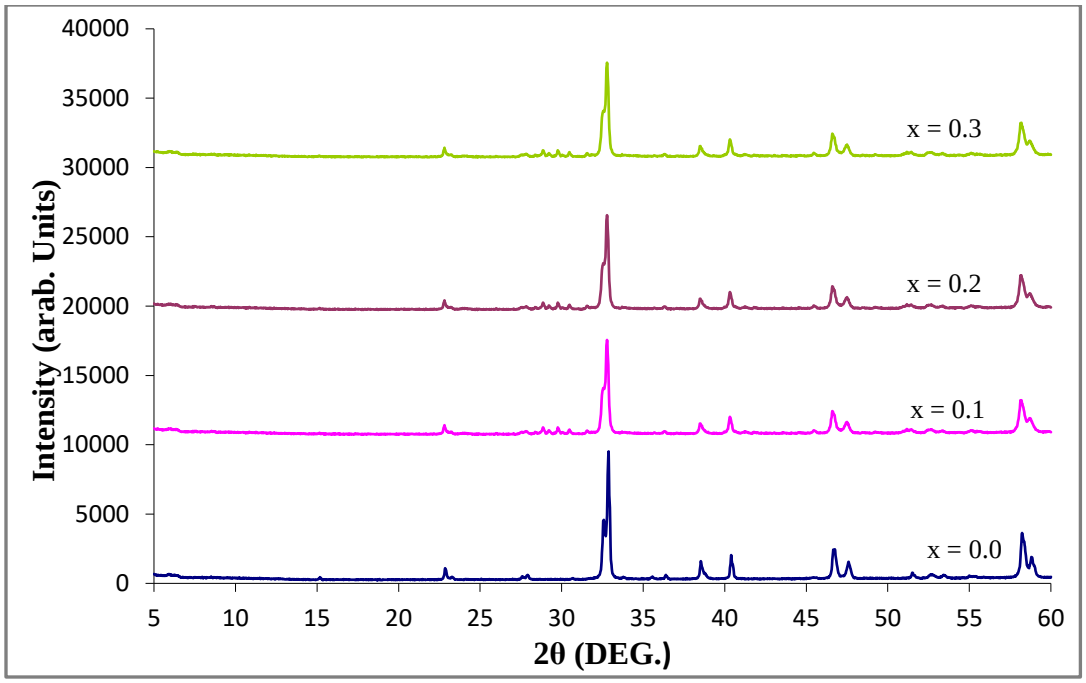

Figure 3 The x-ray powder diffraction pattern using Cu-Kα radiation of x = 0, 0.1, 0.2 and 0.3

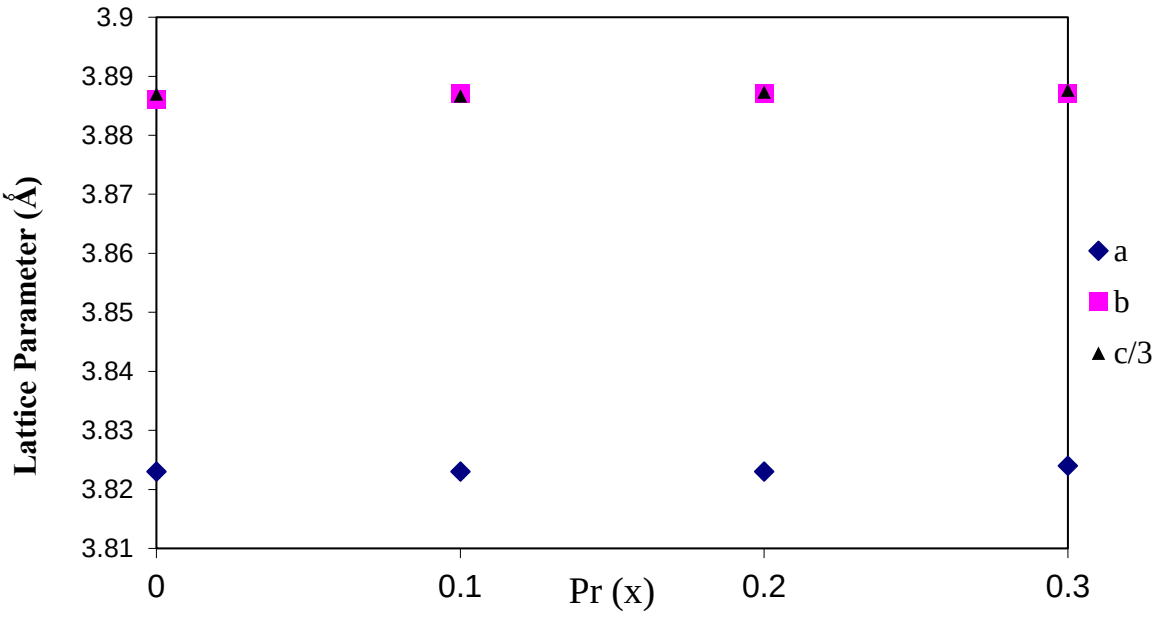

Figure 4 Lattice parameters versus x for the $YBa_2 (Cu_{1-x}Pr_x)_3 O_{7-\delta}$

Table 1 shows the lattice parameters and its unit cell volume. The lattice parameters obtained for x = 0 are a = 3.823 Å, b = 3.886Å and c = 11.66 Å with a unit cell volume of 173.22 $Å^3$. This value agrees with the same sample results reported by Ben et al. (2006) using the standard process prepared samples. For the x = 0.1 sample values obtained for a = 3.823 Å, b = 3.887 Å and c = 11.66 Å and unit cell volume of 173.26 $Å^3$.

Table 1: The lattice parameters a, b, and c, and the unit cell volume

x (Pr)	a (Å)	b (Å)	c (Å)	V($Å^3$)
0.0	3.823	3.886	11.66	173.22
0.1	3.823	3.887	11.66	173.26
0.2	3.823	3.887	11.66	173.29
0.3	3.824	3.887	11.66	173.31

Figure 4 shows that the orthorhombic structure was preserved throughout the substitution range. These results show that our heating process (48 hours at 890-910oC with several intermittent and 24 hours at 890- 910oC in pellets) is suitable to form YPBCO single phase with high quality. However, it is evident that there is no significant effect on the crystal structure by Prx-doping in YBCO within the range of x ($x \leq 0.3$) concentration. The scanning electron micrograph obtained for all samples at 20kV revealed significant similarity in the morphological structure with difference in Prx concentration. Figures 5-8 show the SEM micrograph for x = 0, 0.1, 0.2, and 0.3, respectively. The micrographs reveal several defects, micro-cracks and pores. From the illustrations it is obvious that there was no noticeable change with Prx concentration except for x = 0.0 which agrees with the XRD result shown in Figure 1a. Comparing the pictures, it is obvious that the morphologic features are invariable regardless of Pr-concentration x. We estimated the grain size of the sample and found that the sizes decrease with increase in Pr concentration. For x = 0, 0.1, 0.2, and 0.3 the grained size was 2.0μm, 1.5μm, 1.12μm and 1.14μm, respectively.

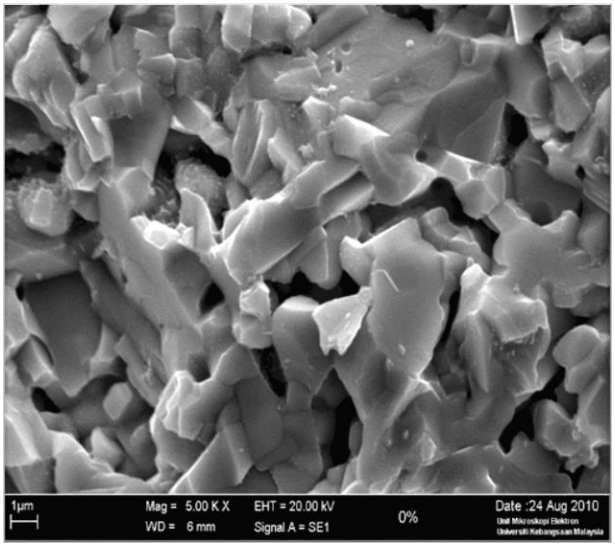

Figure 5 Scanning electron micrograph for $YBa_2(Cu_{1-x}Pr_x)_3O_{7-\delta}$ (x = 0)

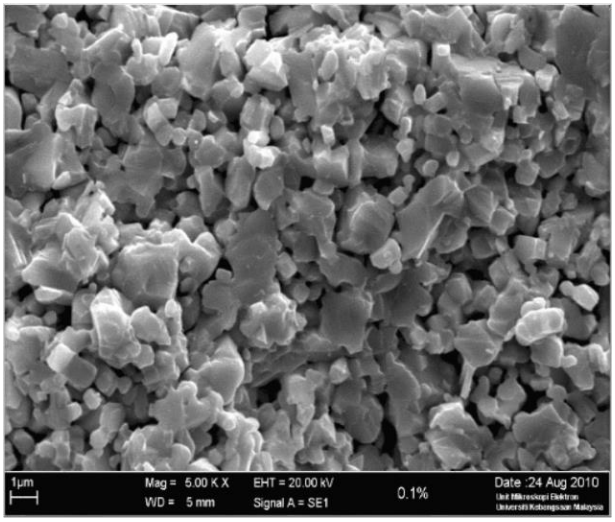

Figure 6 Scanning electron micrograph for $YBa_2(Cu_{1-x}Pr_x)_3O_{7-\delta}$ (x = 0.1)

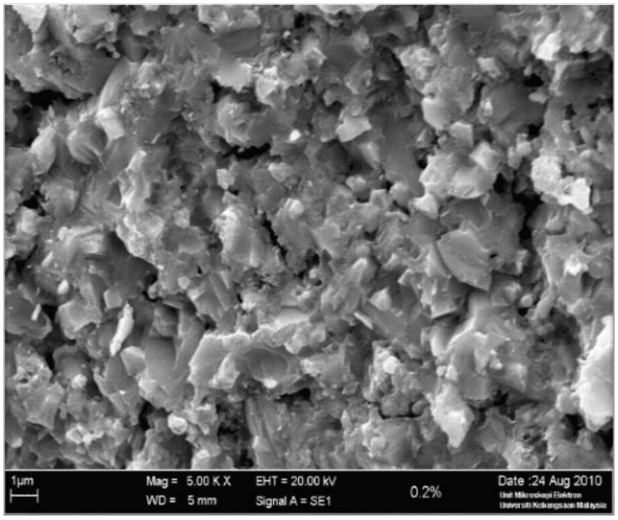

Figure 7 Scanning electron micrograph for $YBa_2 (Cu_{1-x}Pr_x)_3 O_{7-\delta}$ (x = 0.2)

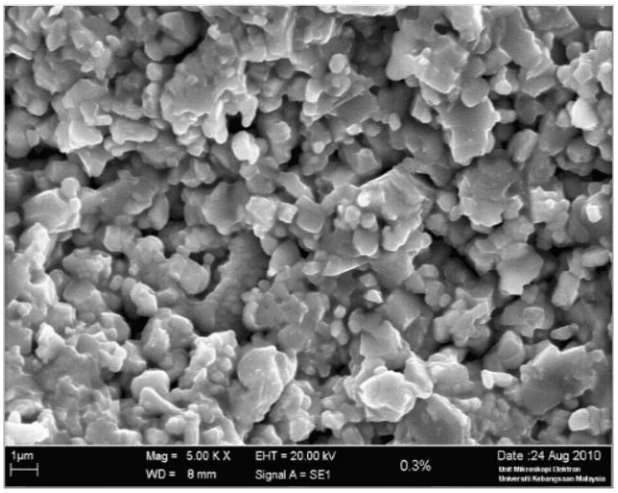

Figure 8 Scanning electron micrograph for $YBa_2 (Cu_{1-x}Pr_x)_3 O_{7-\delta}$ (x= 0.3)

4. Conclusions

The investigation of the effect of Pr_x on microstructure and transitional temperature of $YBa_2 (Cu_{1-x}Pr_x)_3 O_{7-\delta}$ for sample x = 0, 0.1, 0.2, and 0.3 respectively have been studied. Series of $YBa_2 (Cu_{1-x}Pr_x)_3O_{7-\delta}$ samples synthesized using conventional solid state reaction were characterized by means of X-ray diffraction and scanning electron microscopy.

References

[1] Sungho J. Processing and Properties of High-T Superconductors. New York: Pergamum, 1993.

[2] Van Duzer T, Turner CW. Principles of superconductive Devices and Circuits. London: Arnold Press, 1981.

[3] Wu MK, Ashburn JR, Torng CJ, Hor PH, Meng RL, Gao L, Huang ZJ, Wang YQ, Chu CW. Superconductivity at 93 K in a New Mixed-Phase Y-Ba-Cu-O Compound System at Ambient Pressure. Physical Review Letters 1987; 58 (9): 908-910.

[4] Hor PH, Gao L, Meng RL, Huang ZJ, Wang YQ, Forster K, Vassilious J, Chu CW, Wu M K, Ashburn JR Torng CJ. High-pressure study of the new Yb-Ba-Cu-O superconducting compound system. Physical Review Letters 1987; 58 (9): 911-912.

[5] Veal BW, Paulikas AP, You H, Shi H, Fang Y, Downey JW. Observation of temperature-dependent site disorder in $YBa_2Cu_3O_{7-\delta}$ below 150 °C. Physical Review B. 1990; 42(10): 6305-6316.

[6] Sadewasser S, Schilling JS, Paulikas AP, Veal BW. Pressure dependence of T c to 17 GPa with and without relaxation effects in superconducting $YBa_2Cu_3O_x$. Physical Review B. 2000; 61(1):741-749.

[7] Basov, N.G. (edited by). Superconductivity. Lebedev P N. Physics Institute: 86, 178 pgs., Plenum, 1977. ISBN: 0-306-10939-5.

[8] Bardeen J, Cooper LN, Schrieffer JR. Theory of superconductivity. Physical review. 1957; 108 (5): 1175.

[9] John L. Superconductivity: The New Alchemy. London: Contemporary Books Inc., 1st edition, 1989.